Copolymerizations of Tetrafluoroethylene and Perfluoropropylvinyl Ether in Supercritical Carbon Dioxide: Polymer Synthesis, Characterization, and Thermal Properties

Anhou Xu,[1] Wang Zhang Yuan,[1] Junhong Zhao,[1] Hong Li,[1] Heng Zhang,[2] Yongming Zhang[1]

[1]*School of Chemistry and Chemical Technology, Shanghai Jiao Tong University, Shanghai 200240, China*
[2]*Shandong Dongyue Polymer Material Co. Ltd., Zibo 256400, China*

Received 18 February 2011; accepted 7 July 2011
DOI 10.1002/app.35187
Published online 21 October 2011 in Wiley Online Library (wileyonlinelibrary.com).

ABSTRACT: Tetrafluoroethylene (TFE) and perfluoropropylvinyl ether (PPVE) were copolymerized in supercritical carbon dioxide (*sc*-CO_2) with a perfluorodiacyl initiator bis(perfluoro-2-*n*-propoxypropionyl) peroxide (BPPP). The resultant copolymers with stable perfluoroalkyl end groups were obtained, avoiding the decomposition during processing and applications. Reactivity ratios of TFE and PPVE were first reported. The r_{TFE} and r_{PPVE} values are about 8 and 0.08, respectively. Such parameters are significant for the modification of PTFE through copolymerization of TFE and PPVE. It is found that through increasing the reaction pressure from 8.5 to 25 MPa, while r_{TFE} increases by 12.0%, r_{PPVE} decreases by 9.0%, which should be ascribed to the enhancement of the polarity of CO_2 under high pressures. Because the reactivity of TFE is by two orders of magnitude higher than that of PPVE; on one hand, the copolymerization rate falls rapidly with the decrease of TFE feed ratio; on the other hand, TFE content in the copolymer decreases with the reaction time. All copolymers containing different fractions of PPVE enjoy outstanding thermal stability. The DSC result indicates that there exist two forms of crystals with highly regular molecular arrangement or less ordered chain packing which is disturbed by perfluoropropyl pendants. © 2011 Wiley Periodicals, Inc. J Appl Polym Sci 124: 1785–1795, 2012

Key words: copolymerization; fluoropolymers; thermal properties; reactivity ratios; supercritical carbon dioxide

INTRODUCTION

Poly(tetrafluoroethylene) (PTFE) is a semicrystalline fluoroplastic which possesses desirable properties including chemical inertness, biocompatibility, outstanding thermal stability, and low friction coefficient. It has been widely used in the chemical and petrochemical industry, electronics, and biomedical applications.[1–4] However, PTFE is difficult to process and shows weak mechanical properties due to its inherently high crystallinity. Many methods are used to improve its processability and mechanical strengthens, among which copolymerization is often adopted. Perfluoropropylvinyl ether (PPVE) is a common commercial comonomer for TFE. Copolymers of TEE and PPVE, poly(TFE-*co*-PPVE), have been commercialized as Teflon® PFA (DuPont), Aflon® PFA (Asahi Glass), Dyneon® PFA (3*M*/Dyneon), and Neoflon® AP (Daikin). These copolymers not only maintain the advanced functions of PTFE but also display enhanced processability, capable of being shaped with techniques used for thermoplastic polymers.

Poly(TFE-*co*-PPVE) copolymer (PFA) is commercially produced by either emulsion or suspension polymerizations in water. Both processes generate large quantities of wastewater and require huge amounts of energy to dry the resultant polymers. Moreover, the emulsion technique involves perfluoro-octanoic acid (PFOA)-based surfactants, especially for high solid content loadings products. These fluorinated surfactant molecules disperse in the polymer matrix and would migrate gradually during application. Such migration will lead to environmental problems as they are nonbiodegradable and bioaccumulate in human fatty tissues.[5] Additionally, the ionic initiator will also result in the incorporation of thermally unstable carboxylic acid and acid fluoride end-groups[6] which are deleterious to the products during processing and application. Those unstable end-groups would inevitably release certain toxic compounds, such as perfluoroisobutene and hydrofluoride,[7] which are highly harmful to the human body.

Correspondence to: Y. Zhang (ymzsjtu@yahoo.com.cn).
Contract grant sponsor: National Natural Science Foundations of China; contract grant numbers: 20504020, 50673057.
Contract grant sponsor: Shanghai Leading Academic Discipline Project; contract grant number: B202.

Regarding this, new techniques based on supercritical fluid have attracted much attention in the field of polymer synthesis.[8,9] Particularly, supercritical carbon dioxide (*sc*-CO_2) is of tremendous interest in the syntheses of polymers as it is cheap, facile to obtain, inflammable, and environment friendly. What's more, polymers can be isolated from the reaction mixture via simple depressurization, resulting in clean and dry polymer products.[10,11] Specifically, mixing TFE with CO_2 dramatically improves the safety of handling the monomer.[12] In the fluoropolymer industry, DuPont has recently commercialized certain grades of Teflon® products based on CO_2 technology,[13] offering superior properties to those materials prepared conventionally.

Recently, copolymerization of TFE and PPVE in *sc*-CO_2 has been reported.[14,15] It is demonstrated that *sc*-CO_2 is an excellent solvent for TFE-based copolymer syntheses, which generally produce polymers with high molecular weights in good yields, and less deleterious end groups as compared to those obtained in aqueous emulsion polymerizations. Up to date, however, there is not enough information reported on the copolymerization of TFE and PPVE in *sc*-CO_2, including polymerization rates, pressure effect, polymerization behaviors, and even the basic monomer reactivity ratios. One characteristic of using supercritical fluids as reaction media is that slight changes in the pressure afford great differences in the density-dependent bulk solvent properties, such as dielectric constant and viscosity, which have strong influence on the monomer reactivity ratios.[16,17] Pressure effect on polymer yields and molecular weights in supercritical fluid were also reported.[18,19] Following previous works, we carefully studied the free radical copolymerization of TFE and PPVE initiated by a perfluorodiacyl peroxide initiator, bis(perfluoro-2-*n*-propoxypropionyl) peroxide (BPPP) in *sc*-CO_2. Determination of the monomer reactivity ratios, the copolymerization behaviors, pressure effect, and thermal properties of the polymers are investigated.

EXPERIMENTAL

Materials

Both TFE (>99.999%) and PPVE (>99.9%) were supplied by Shandong Dongyue Polymer Materials Co. Ltd. (Zibo, China) and used without further purification. CO_2 (99.99%, oxygen content $\leq$10 ppm) was supplied from Zibo Baiyan Gases company. PFC-8, $C_3F_7OCF(CF_3)CF_2OCF_2CF_3$, a low-boiling perfluorinated solvent was kindly provided by Shandong Dongyue Shenzhou New Material Co. Ltd. and used as received. BPPP initiator $[C_3F_7OCF(CF_3)COO]_2$ was synthesized according to the reported procedure[20] in PFC-8. A PFC-8 solution of BPPP ($\sim$ 5%) was stored in a dry-ice bath in the dark. An iodimetry technique, ASTM Method E 298-91, was utilized to determine the initiator concentrations in solutions. Both PTFE and PPPVE were prepared in *sc*-CO_2 with BPPP initiator. After being dried, PTFE with a molecular weight of 210 kg/mol and PPPVE homopolymer were obtained as powders and sticky glue, respectively.

Copolymerization of TFE and PPVE in *sc*-CO_2

Copolymerization was conducted in a 100-mL high pressure reactor equipped with a magnetic stirring bar, a thermocouple, and a rupture disk. The reactor was immersed in a water bath. In a typical experiment, the reaction system was sealed and evacuated. Then, the base of the reactor was chilled to well below 0°C using a liquid nitrogen bath. Meanwhile, chilled PPVE (−10°C) was added to a test pipe and transferred to the evacuated reactor by cannula. After being charged with TFE/CO_2 mixture ($\sim$ 50 wt %) under stirring, the reactor was heated to a fixed reaction temperature and further filled with CO_2 (using an air driven gas booster SC, Model GB-30) to achieve a pressure lower than the desired reaction pressure by 2–3 MPa. Then, PFC-8/BPPP solution was added through a high-pressure tube. The tube was further purged with CO_2 until the reactor was brought to the desired pressure. After reaction for designed time, the reactor was cooled to 0°C by liquid nitrogen (less than 2 min for cooling from 35 to 0°C). The polymerizations were stopped in a short time (10–20 min) at low monomer conversions, aiming to calculate the monomer reactivity ratios. After CO_2 was slowly released, the powdery product was collected and dried under vacuum at 80°C for $\geq$12 h to remove volatile compounds.

Characterization

Solid-stated ^{19}F-NMR spectra were measured on a Bruker Ultrashield 400 Plus spectrometer operating at a resonance frequency of 376 MHz for ^{19}F. All fluorine chemical shifts were referred to external $CFCl_3$ set to 0 ppm. FT-IR spectra of hot-pressed thin polymer films were taken on a Bruker Tensor-27 for 32 scans with a resolution of 4 cm^{-1}. Differential scanning calorimetry (DSC) measurements of poly(TFE-*co*-PPVE) copolymers were conducted on a TA Instrument DSC-Q100. The scanning temperature ranges from −50 to 380°C for each sample with a heating or cooling rate of 10°C min^{-1}. Thermal gravimetric analysis (TGA) was performed on a TA Q50 instrument under nitrogen with a heating rate of 10°C min^{-1} and scanning range of 40–800°C. The X-ray diffraction (XRD) measurements were carried

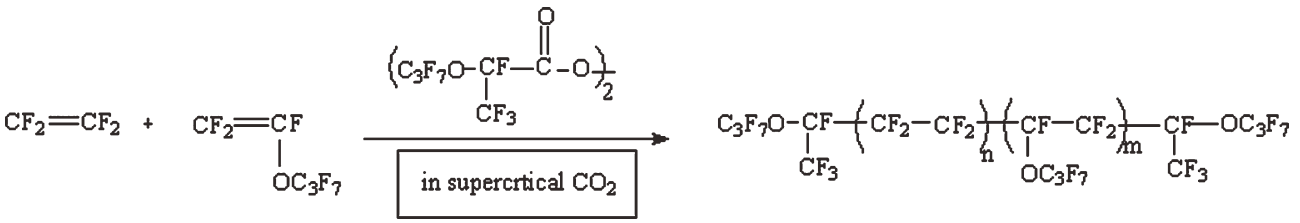

Figure 1 Synthesis of poly(TFE-*co*-PPVE) with perfluoroalkyl end groups initiated by BPPP in *sc*-CO_2.

out on a Rigaku D/Max-3C diffractometer (Rigaku, Japan) equipped with a rotating anode and a Cu Kα radiation source ($\lambda = 0.15418$ nm) operated at 40 kV and 30 mA, at a scanning rate of 4° min^{-1}.

RESULTS AND DISCUSSION

Copolymerization

TFE and PPVE were copolymerized in *sc*-CO_2 to produce poly(TFE-*co*-PPVE) with perfluoroalkyl end groups using BPPP as initiator (Fig. 1). The copolymer compositions are calculated from corresponding ^{19}F-NMR spectra, and the results are summarized in Table I. Clearly, for the same reaction time, higher initial PPVE concentration results in more PPVE segment fraction in the resulting copolymer.

Structure characterization

Spectroscopic techniques were employed to characterize the structures of the polymeric products. All the polymers give satisfactory analysis data corresponding to their expected structures. The typical IR spectrum of PTFE and poly(TFE-*co*-PPVE) (taken from Table I, entry 3) are given in Figure 2(A). The copolymer shows absorption bands at 994 and 1333 cm^{-1}, which are assignable to the stretching vibrations of C—O—C and —CF⟨,[7,21] respectively. These bands are absent in the spectrum of PTFE, thus verifying the incorporation of PPVE monomer units in the resulting polymer. Such prominent absorbance at 994 cm^{-1}, which is the most characteristic feature for the copolymer, becomes more and more remarkable from PFA1 to PFA5 [Fig. 2(B)], indicating the increased fraction of PPVE, which is consistent with the calculated results. Another peak at 2365 cm^{-1} can be ascribed to the combination overtone from the bands of 1152 and 1213 cm^{-1}.[22] Meanwhile, the magnified inset panel in Figure 2(A) shows no absorption bands at 1777, 1812, and 1883 cm^{-1}, suggesting the absence of unstable carboxylic acid or acid fluoride end groups in the copolymers.[23,24]

Formation of the poly(TFE-*co*-PPVE) copolymer is also confirmed by the solid stated ^{19}F-NMR spectra. Figure 3 depicts the typical ^{19}F-NMR spectrum of poly(TFE-*co*-PPVE) copolymer. For comparison, the spectrum of PPVE is also given in the same figure. As can be seen from Figure 3(A), all the peaks are well reserved and can be reasonably assigned according to the structure of PPVE.[25] For example, the signals at −81 and −86 ppm can be assigned to the OCF_2 and CF_3 groups, respectively. The corresponding signals for poly(TFE-*co*-PPVE) copolymer appear at about −81 and −83 ppm [Fig. 3(B)].[23] While the absorption peak at about −136 ppm is ascribed to the CF group in PPVE, a weak signal at the same position in the copolymer backbone due to the incorporation of PPVE is observed, as suggested previously.[23,26] By comparison with the signals in PPVE, the peak near −130 ppm in the copolymer can be assigned to the fluorines of CF_2 connected to the CF_3 group.[23] Additionally, the weak peak at −142 ppm[27] is the absorption of CF group in the initiator fragment —C*F*(CF_3)$OCF_2CF_2CF_3$. As both TFE

TABLE I
Copolymerizations of TFE and PPVE in *sc*-CO_2[a]

Entry	Feed ratio (mol %) TFE	Feed ratio (mol %) PPVE	Time (min)	Copolymer composition (mol %) TFE	Copolymer composition (mol %) PPVE	Conversion[b] (wt%)	Sample name
1	96.7	3.3	10	99.6	0.4	3.1	PFA1
2	91.3	8.7	10	98.9	1.1	2.9	PFA2
3	87.7	12.3	15	98.4	1.6	3.9	PFA3
4	79.1	20.9	15	96.8	3.2	2.6	PFA4
5	74.3	25.7	20	95.8	4.2	2.2	PFA5

[a] Carried out at 35°C under an initial vessel pressure of 13 MPa; the total initial monomer and initiator concentrations ($[M]_0$ and $[BPPP]_0$) are 0.8 and 4×10^{-4} M, respectively.
[b] The conversion was defined as the weight percentage of the resulting copolymer to the total amount of monomers.

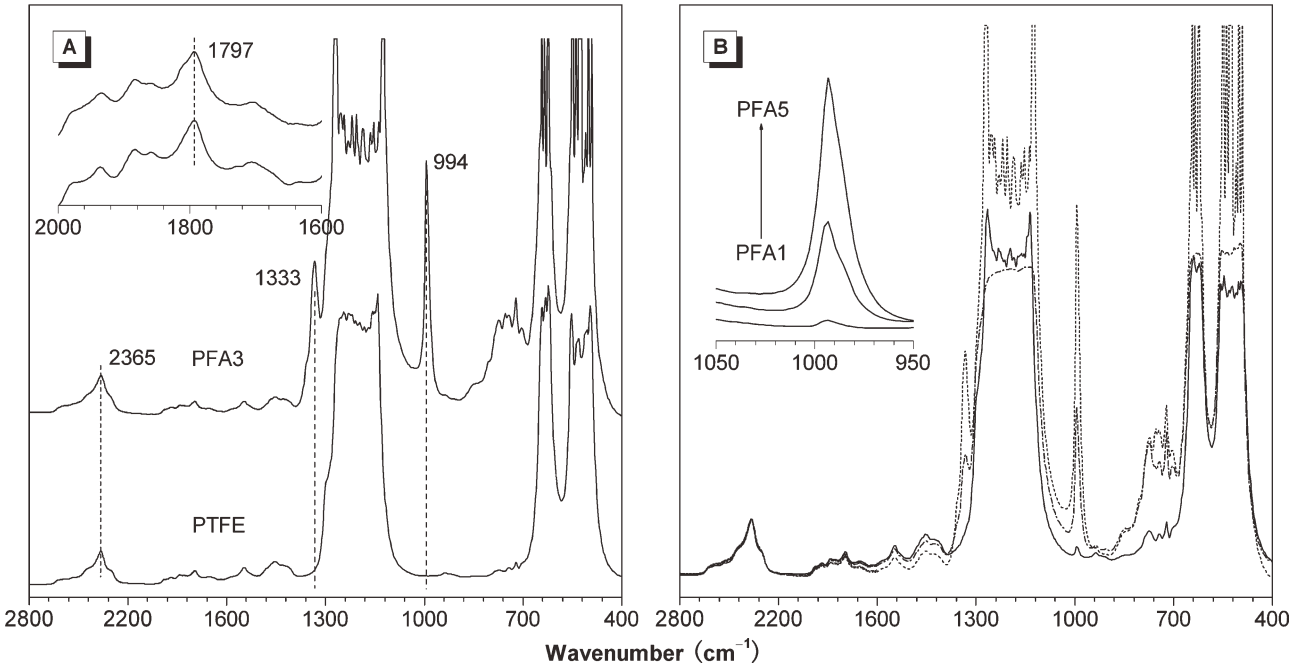

Figure 2 FT-IR spectra of (A) poly(TFE-*co*-PPVE) (sample taken from Table I, entry 3) and PTFE and (B) PFA1, PFA3, and PFA5 with different PPVE fractions.

and PPVE units contain CF_2 segments, a dominant peak at −122 ppm corresponding to the absorption of —CF_2— is observed. The PPVE content in the copolymers was determined using the peak area integrations of —C*F*⟨ and —CF_2— groups in PPVE and TFE units, respectively.

To further prove the formation of copolymers and rule out the possibility of generating a fraction of mixture of two homopolymers, a physical mixture of PTFE and PPPVE homopolymers with the composition of 96.7/3.3 mol % (91.7/8.3 wt %), which is comparable to that of the copolymer obtained in Table I, entry 4, was prepared. TGA measurement indicates that there is only one weight losing stage for poly(TFE-*co*-PPVE), but two for the physical blend (Fig. 4). Clearly, while PPPVE homopolymer in the blend first starts to decompose when attacked by thermolytic species, its PTFE counterpart is kept intact until PPPVE is burned completely, and then it began to lose weight at 461°C at the weight loss of 9 wt %, which is well consistent with the weight percentage of PTFE in the blend. However, when it comes to the poly(TFE-*co*-PPVE) copolymer, it started to lose weight at 360°C with only one stage, thus suggesting the homogenous and random distribution of TFE and PPVE segments in the copolymer chains. The TGA thermograms of the homopolymers PTFE and PPPVE are also given in Figure 4 for comparison. The initial and terminative decomposition temperatures of 461 and 374°C are found for PTFE and PPPVE, respectively, which agree well with those obtained in their physical mixture.

To eliminate the possibility of generating a fraction of the PTFE homopolymer, two samples, poly(TFE-*co*-PPVE) (sample taken from Table I, entry 4) as well as a physical mixture of poly(TFE-*co*-PPVE) (90 wt %) and PTFE (10 wt %), are also analyzed by DSC (Fig. 5). The DSC curve of the physical mixture shows two more peaks (328 and 310°C) when compared with that of poly(TFE-*co*-PPVE). Clearly, a small fraction of PTFE in the physical mixture can generate obvious peaks since PTFE is a high crystallinity polymer possessing large enthalpy changes during melting and crystallization.[28] The DSC curve of poly(TFE-*co*-PPVE) copolymer has four peaks (280/316, 265/296°C) belonging to its melting and crystallization transitions, respectively, indicating that there is no detectable PTFE homopolymer in the poly(TFE-*co*-PPVE) copolymer product.

BPPP was used as the initiator during the polymerization process to produce copolymers with stable perfluoroalkyl end groups. The dissociation of BPPP proceeds via a single bond homolysis mechanism,[29] resulting in the formation of perfluoroalkyl radicals which further initiate the monomers to copolymerize. For such a system, it is generally accepted that termination occurs by combination, which is proved by the absence of the absorption peaks of —CF=CF_2 at 1784 cm^{-1} and −90.7 ppm[30] in the IR and ^{19}F-NMR spectra of poly(TFE-*co*-PPVE), respectively. Termination by transfer or disproportionation reaction did not occur at a detectable extent. It should be ascribed to the high electrophilicity of fluorinated free radicals, which is

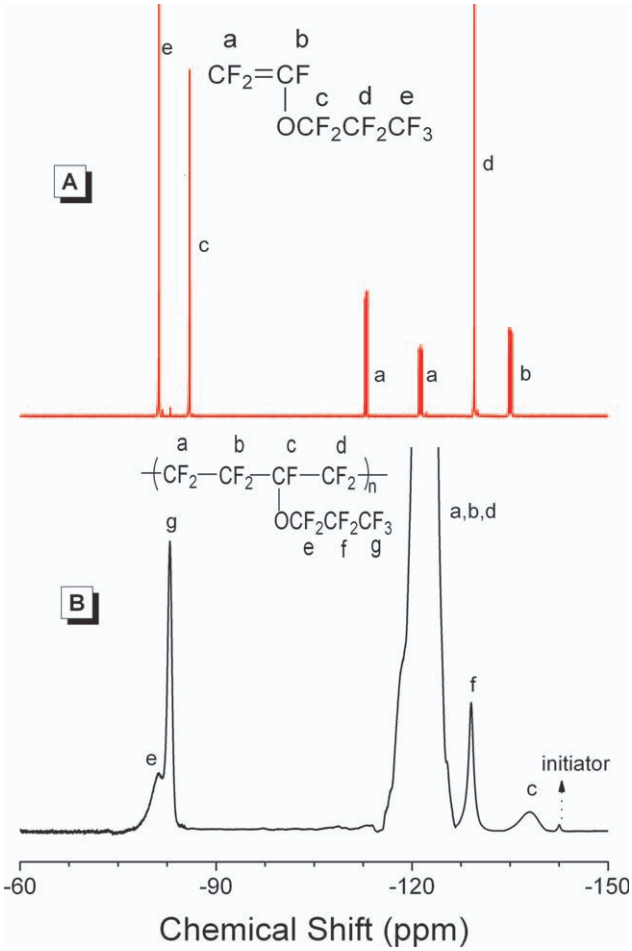

Figure 3 ^{19}F-NMR spectra for (A) PPVE monomer and (B) poly(TFE-*co*-PPVE) (sample taken from Table I, entry 3). [Color figure can be viewed in the online issue, which is available at wileyonlinelibrary.com]

difficult to abstract fluorine from monomers or polymers. Meanwhile, since hydrogen-containing impurities were strictly excluded from the polymerization recipe, no hydrogen-bearing ends would be expected. So, the end groups of the copolymers should be $C_3F_7OCF(CF_3)$— perfluoroalkyls, as illustrated in Figure 1. It is so important for fluoropolymers to have such stable end groups, since they are normally melt processed at high temperature (more than 400°C).[7] Otherwise, active end groups can undergo decomposition to form bubbles, discoloration, and erratic molecular weight changes in the final products, which should be avoided in terms of their long-term applications.

Determination of the monomer reactivity ratios

Monomer reactivity ratios are important parameters for copolymerizations. They are extremely useful for tailoring copolymer compositions for a diversity of applications. Due to its environmental friendly characteristic and the facility of removing highly toxic

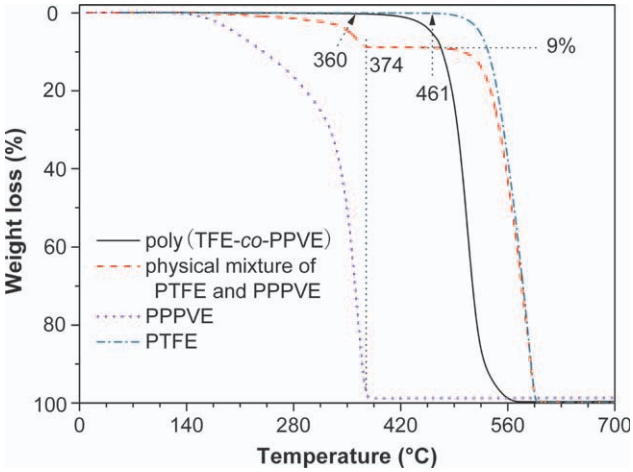

Figure 4 Thermograms of poly(TFE-*co*-PPVE) (96.7 mol % TFE, sample taken from Table I, entry 4); a physical mixture of PTFE and PPPVE homopolymers (96.8 mol % TFE), PPPVE, and PTFE. [Color figure can be viewed in the online issue, which is available at wileyonlinelibrary.com]

initiator residues and decomposition products in it, *sc*-CO_2 is widely used in the synthesis of fluoropolymers. It is, therefore, of critical importance for us to explore the monomer reactivity ratios of TFE and PPVE in *sc*-CO_2. Many analytical methods have been developed to evaluate the monomer reactivity ratios, among which Kelen-Tudos (K-T) method[31] is widely used due to its advantages over other approaches. Herein, we used the K-T method to determine monomer activities of TFE and PPVE. We also adopted this method because it can be applied even at extreme experimental conditions, including largely mismatched monomer reactivity ratios and

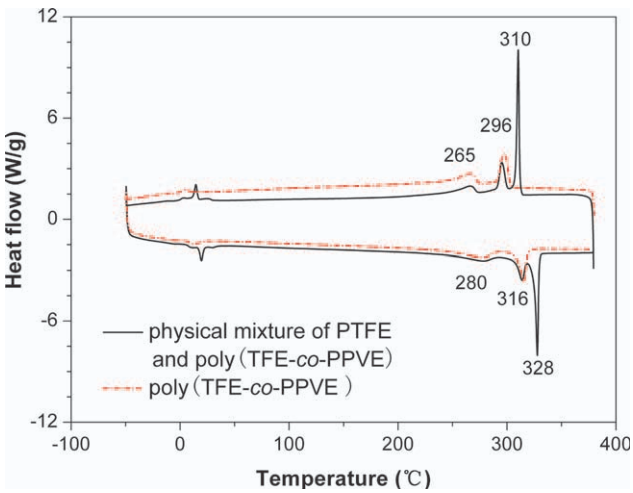

Figure 5 Differential scanning calorimetry (DSC) curves of poly(TFE-*co*-PPVE) (96.8 mol % TFE, sample taken from Table I, entry 4) and the physical mixture of PTFE (10 wt %) with the copolymers (90 wt %). [Color figure can be viewed in the online issue, which is available at wileyonlinelibrary.com]

rather low concentration of one monomer. The K-T method is based on the following equation:

$$\eta = \left(r_1 + \frac{r_2}{\alpha}\right)\xi - \frac{r_2}{\alpha} \quad (1)$$

where r_1 and r_2 are monomer activity ratios, η and ξ are functions of parameters G and H:

$$\eta = G/(\alpha + H) \quad \text{and} \quad \xi = H/(\alpha + H) \quad (2)$$

and α is a constant equal to $(H_{max}H_{min})^{1/2}$, H_{max} and H_{min} being the maximum and minimum H values, respectively, from the series of measurements. The parameters G and H are defined as below:

$$G = f^*[(F-1)/F] \quad \text{and} \quad H = f^2/F \quad (3)$$

with

$$f = m_1/m_2 \quad \text{and} \quad F = M_1/M_2 \quad (4)$$

where m_1 and m_2 are the monomer molar feed fractions, and M_1 and M_2 are the copolymer molar compositions. Thus, based on above equations, a linear plot of η versus ξ gives directly r_1 and $-r_2/\alpha$ at $\xi =$ 1 and 0, respectively.

The linear extrapolation plot using the K-T method is depicted in Figure 6, and the reactivity ratios for TFE (r_{TFE}) and PPVE (r_{PPVE}) in *sc*-CO_2 at 13 MPa are 8.63 and 0.083, respectively, suggesting that the radicals on TFE homopolymerize more readily than its copolymerizing with PPVE, whereas the radicals on PPVE primarily cross-propagate with TFE.

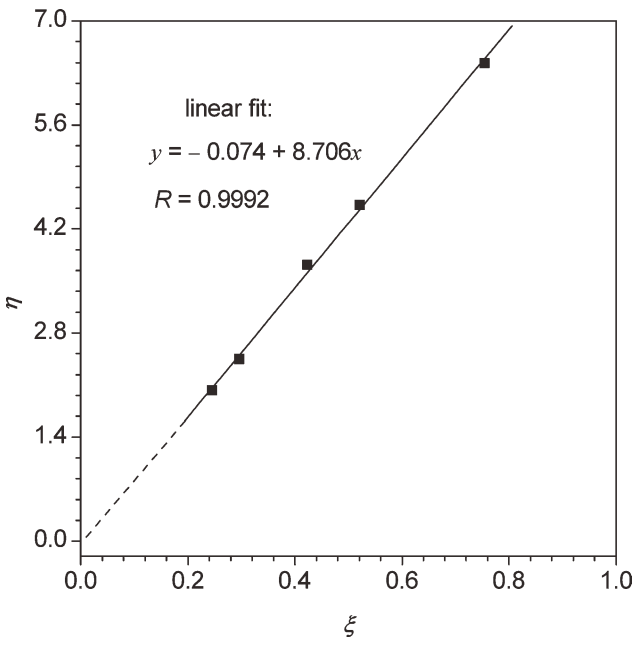

Figure 6 K-T plot for determining the monomer reactivity ratios in the copolymerization of TFE and PPVE in *sc*-CO_2 at 13 MPa.

TABLE II
Effect of Reaction Pressure on r_{TFE} and r_{PPVE} in *sc*-CO_2

Pressure (MPa)	Density (g mL^{-1})	Dielectric constant ε (35°C)	r_{TFE}	r_{PPVE}	r_{TFE} r_{PPVE}
8.5	1.37	1.27	7.91	0.087	0.688
13	1.79	1.48	8.63	0.083	0.716
25	1.99	1.55	8.86	0.079	0.700

The effect of pressure on reactivity ratios was also studied. The copolymerizations of TFE and PPVE were carried out under another two pressures of 8.5 and 25 MPa, respectively. The monomer reactivity ratios were calculated according to Eq. (1). The results are summarized in Table II. Clearly, by increasing the reaction pressure from 8.5 to 25 MPa, while r_{TFE} is improved from 7.91 to 8.86, r_{PPVE} is decreased from 0.087 to 0.079, the increase and decrease in amplitudes are 12.0% and 9.2%, respectively, revealing the striking pressure effect on reactivity ratios in such system.

The differences in reactivity ratios of the monomers at various pressures can be ascribed to the changes of polarity of reaction medium, as reported by Baradie and Shoichet,[32] and preferential solvation of a monomer in *sc*-CO_2 will be enhanced by the differences in the polarity of the solvent and the monomers; the polar monomer is pushed by the nonpolar *sc*-CO_2 solvent from the solution phase to the polymer phase. Because of its unsymmetrical structure, PPVE enjoys higher polarity than TFE. For the *sc*-CO_2 reaction media, when the pressure was increased from 8.5 to 25 MPa, its dielectric constant improved from 1.27 to 1.55,[33] suggesting the enhancement of polarity. Hence, the difference in polarity between *sc*-CO_2 and TFE enlarged, whereas that between CO_2 and PPVE decreased, thus making TFE much easier and PPVE less likely to come into the polymer phase. Therefore, higher r_{TFE} and lower r_{PPVE} values are observed when the pressure of *sc*-CO_2 is increased. The effect of solvent polarity on the reactivity ratios is not a sole phenomenon for TFE and PPVE occurring in *sc*-CO_2. A similar effect was also observed in the solution copolymerizations of styrene and 2-hydroxyethyl methacrylate in different solvents.[34]

Effect of TFE/PPVE feed ratio

Copolymerizations and monomer feed ratios will greatly affect the copolymerization rates and resulting copolymer compositions. To evaluate such an effect for TFE and PPVE in *sc*-CO_2, copolymerization rates with different monomer feed ratios under

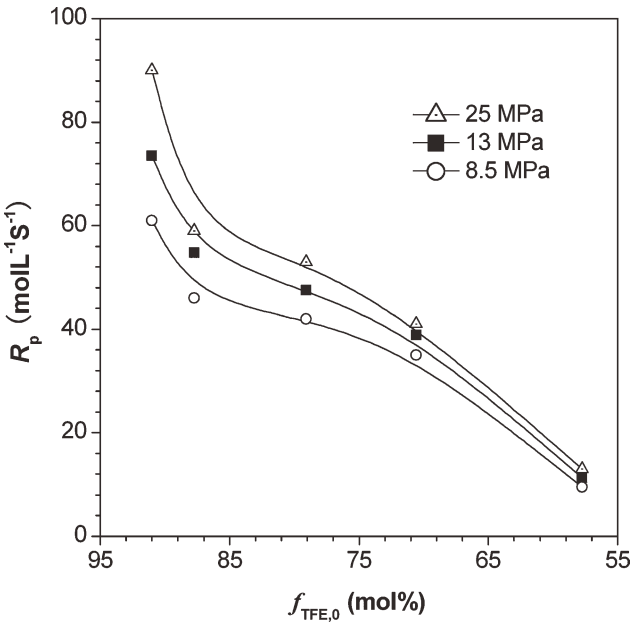

Figure 7 Plots of copolymerization rate versus initial feed ratio of TFE ($f_{TFE,0}$) in *sc*-CO_2 under different pressures. Temp. = 35°C, $[M]_0$ = 0.8 M, $[BPPP]_0$ = 0.4 m*M*, reaction time = 60 min.

varied pressures were determined gravimetrically from the conversion according to Eq. (5)

$$R_p = \frac{\text{conv}}{\Delta t_p} \tag{5}$$

where R_p, Δt_p, and conv are copolymerization rate, polymerization time, and monomer conversion, respectively. The results are depicted in Figure 7. Evidently, with decreased feed ratio of TFE, the copolymerization rate fell sharply, indicating that R_p is mainly dependent on the concentration of TFE. This phenomenon is concordant with r_{TFE} and r_{PPVE} values derived from the K-T method. In any case, r_{TFE} (≈8) is higher than r_{PPVE} (≈0.08) by almost two orders of magnitude, resulting in R_p being mainly determined by the reactivity of TFE, whose polymerization rate is monotonically decreasing with its declined concentration. Meanwhile, the pressure effect on R_p was also checked. As revealed in Figure 7, under identical conditions, higher pressures give higher R_p values, which should be ascribed to the increased r_{TFE} under elevated pressures.

Copolymer composition is another important parameter involved in copolymerization. Figure 8 displays the copolymer composition data obtained at different monomer feed ratios under various pressures. The theoretical compositions calculated by the Mayo-Lewis equation are also given in the same figure for comparison.[35] It is evident that the data well agree with each other. It is also noticeable that the percent of TFE segments in the copolymer chain is always higher than its corresponding feed fraction, which is consistent with the characteristic of typical nonideal copolymerization ($r_{TFE} > 1$, $r_{PPVE} < 1$, and $r_{TFE} \cdot r_{PPVE} < 1$, also see Table II).

Effect of reaction time

The relations between reaction time and conversion of TFE and PPVE in *sc*-CO_2 with two TFE feed fractions ($f_{TFE,0}$) of 91.3 and 71.4 mol % (35°C, 13 MPa) are presented in Figure 9. The conversion increased dramatically within 1 h, then rose up slightly and leveled up eventually after another 2 h. Such results are well consistent with the first-order decomposition feature of BPPP initiator. It is known that the half-life ($t_{1/2}$) of BPPP at 35°C is about 45 min,[29] thus after 90 min ($2 \times t_{1/2}$), over 75% of BPPP was consumed, thus continuous heating impacted little on the monomer conversions.

When one of the monomer reactivity ratios, r_1 or r_2, is larger than 1, and the other is smaller than 1, a considerable composition shift can be observed during the copolymerization process. Then, copolymer composition will be appreciably different from the initial one. Such behavior is attributed to the higher reactivity of one monomer. Consequently, more units of this monomer will be inserted in the macromolecular chain, giving a significant tendency of the formation of block-like segments. For poly(TFE-*co*-PPVE) system, r_{TFE} (≈8) and r_{PPVE} (≈0.08) are much greater and less than 1, respectively. Such reactivity ratio values suggest that the growing radicals with both TFE and PPVE ends prefer to be added to TFE

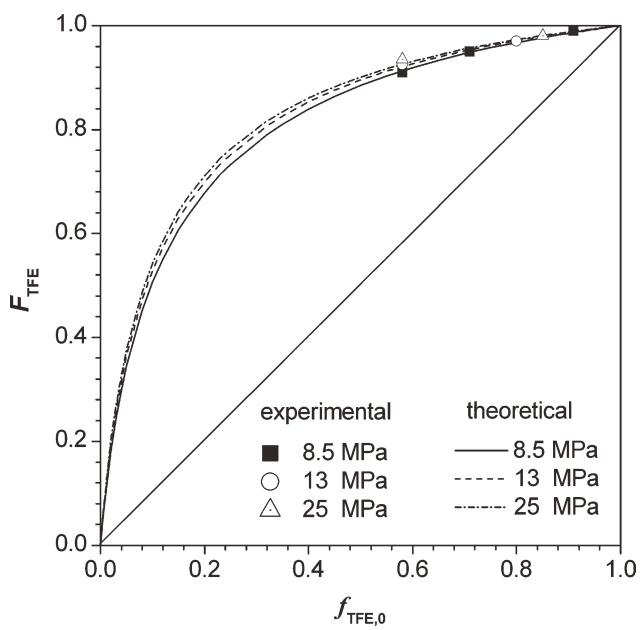

Figure 8 Copolymerization diagram for TFE and PPVE in *sc*-CO2 with different pressures. Temp. = 35°C, $[M]_0$ = 0.8 M, $[BPPP]_0$ = 0.4 m*M*, reaction time = 60 min.

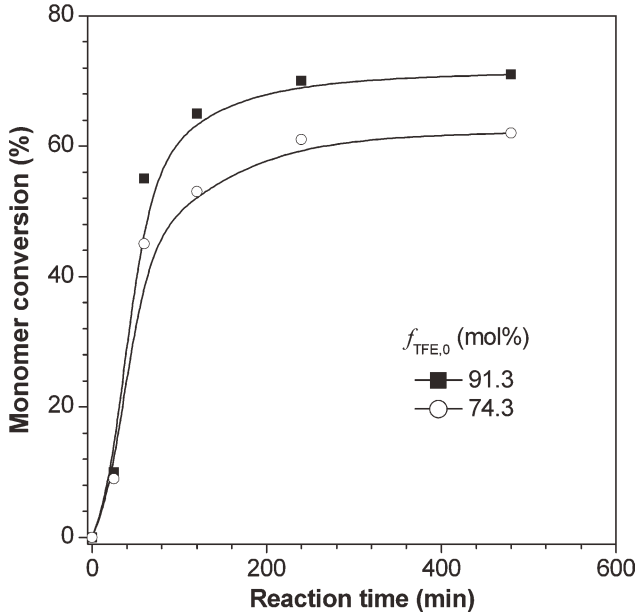

Figure 9 Plots of monomer conversion versus reaction time with different TFE feed ratios in *sc*-CO2. Temp. = 35°C, initial vessel pressure = 13 MPa, $[M]_0 = 0.8M$, $[BPPP]_0 = 0.4$ m*M*.

at a much higher rate than to PPVE. The large difference in the reactivity ratios of TFE and PPVE also predicts a high tendency to form blocky runs. Therefore, with prolonged reaction time, less and less mole fraction of TFE would be resided in the reaction system, and the TFE content in the copolymer would decrease gradually with monomer conversions. Meanwhile, the block length of TFE units would be shorter and shorter with prolonged reaction time. This evolution of the copolymer composition is illustrated in Figure 10, in which experimental data and theoretical curves based on Skeist equation (Eq. (6)) are given out.

$$\ln(1 - \text{conv}) = \int_{f_{TFE,0}}^{f_{TFE,t}} df_{TFE}/(F_{TFE} - f_{TFE}) \qquad (6)$$

Instantaneous F_{TFE} is expressed on the basis of the Mayo and Lewis equation including f_{TFE}, r_{TFE}, and r_{PPVE}, for each infinitesimal interval of feed composition. By numerical integration, compositions of the residual monomers ($f_{TFE,t}$) and copolymer (F^*_{TFE}, Eq. (7)) at a given comonomer conversion can be determined. Figure 10 shows that with improved monomer conversions, F^*_{TFE} decreased gradually, and the experimental evolution of the copolymer composition is in good agreement with the theoretical prediction by Skeist equation (Eq. (6)).

$$F^*_{TFE} = [f_{TFE,0} - f_{TFE,t} \times (1 - \text{conv})]/\text{conv} \qquad (7)$$

Thermal properties

Most fluoropolymers are melt processed under high temperatures. It is thus important to investigate their thermal properties. We first examined the thermal stability of the copolymers by TGA under nitrogen. Temperature for 5 wt % loss has often been used as a degradation temperature (T_d) to estimate thermal stability of a synthetic polymer. As shown in Figure 11, these PFA products exhibit good thermal stability, and all the copolymers have the T_d values above 438°C. It is understandable that both perfluorinated main chains and perfluoroalky end groups endowed resultant copolymers with good stability under higher temperatures. To inspect the early thermogravimetry process where weight loss would be related with polymer end groups,[36] the temperatures for 1 wt % loss (T_1) for these PFA copolymers are also obtained. The results show that all T_1 values are higher than 415°C, similar to normal commercial Hyflon® PFA (T_1 = 420–440°C) which has been dealt with fluorination. Besides the adopted perfluorinated initiator, the higher T_1 values can be also explained considering that because of the ability of CO_2 to plasticize polymeric materials and its excellent transport properties, β-scission reaction is suppressed relative to polymer propagation, thereby yielding less unstable groups.[37] Furthermore, surfactant-free strategy also helps, because fluoropolymer product prepared with surfactant-assisted polymerization in *sc*-CO_2 should show obvious thermal degradation in the temperature interval from 140 to 240°C.[38]

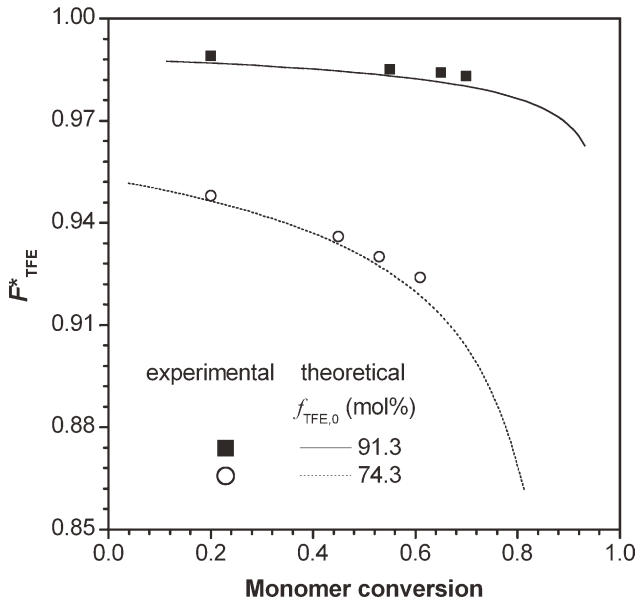

Figure 10 Dependence of the copolymer composition (F^*_{TFE}) on monomer conversions with different monomer feed ratios in *sc*-CO_2. Temp. = 35°C, initial vessel pressure = 13 MPa, $[M]_0 = 0.8$ M, $[BPPP]_0 = 0.4$ m*M*.

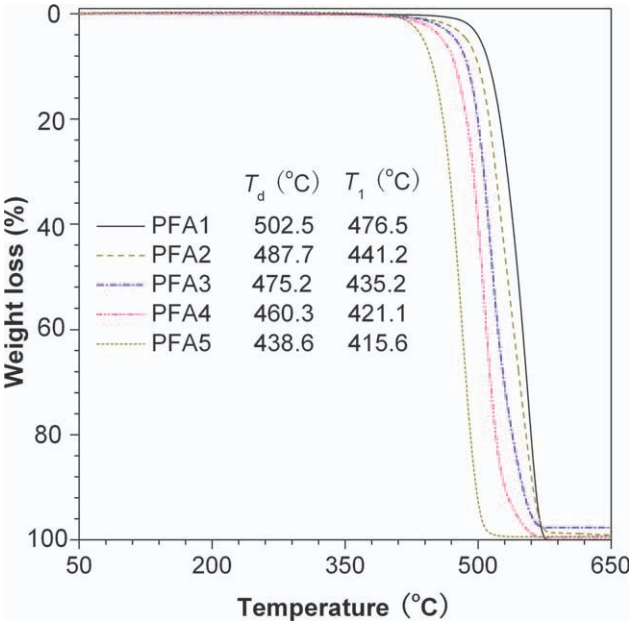

Figure 11 TGA thermograms of PFA1∼PFA5 synthesized in *sc*-CO_2 measured under nitrogen at a heating rate of 10°C min^{-1} [Color figure can be viewed in the online issue, which is available at www.interscience.wiley.com].

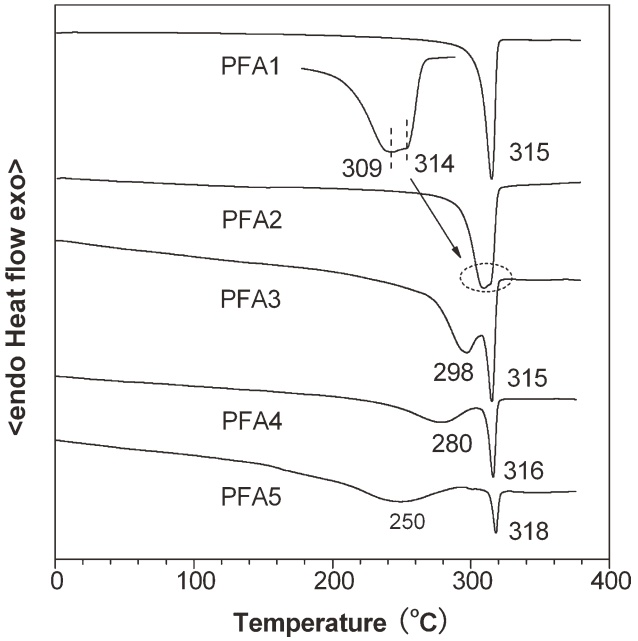

Figure 12 DSC thermograms of PFA1∼PFA5 synthesized in *sc*-CO_2 measured under nitrogen at a scan rate of 10°C min^{-1}.

Because of their high thermal stability, we further investigated the transition behaviors of PFA1 ∼ PFA5 through DSC measurement. Figure 12 depicts the DSC thermograms of PFA1 ∼ PFA5 with different compositions obtained in *sc*-CO_2. When PPVE content is merely 0.4 mol % (PFA1), only one sharp peak at 315°C corresponding to the melting transition of PFA1 is observed, indicating the existence of only one kind of crystal in the copolymer. With an increase of PPVE content, the melting peak becomes broad (PFA2, f_{PPVE} = 1.1 mol %), and closer inspection reveals that it is an overlap of two peaks at 309 and 314°C, suggesting the presence of new crystalline moieties. Further enhancement of PPVE fraction gives two distinct peaks locating at 298/315, 280/316, and 250/318°C for PFA3, PFA4, and PFA5, respectively. Obviously, with increased PPVE content, while the high temperature transition exhibits little change, the low temperature transition shifts to a much lower side. It is reported previously that perfluoropropyl side chains cannot be incorporated into the PTFE crystalline phase.[39,40] Therefore, the DSC results indicate that there are two forms of crystals existing in the copolymers. One is in higher

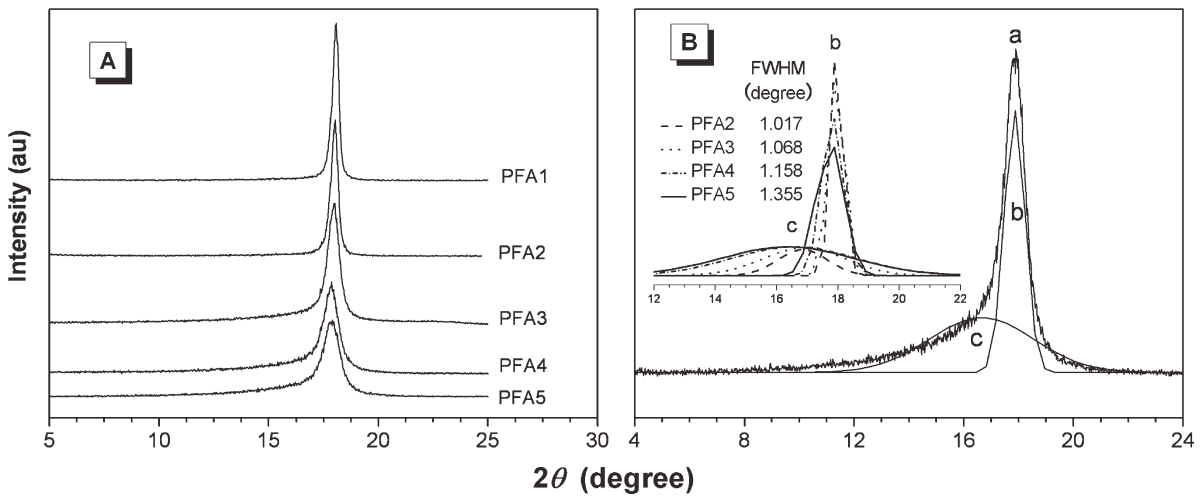

Figure 13 (A) XRD profiles of PFA1 ∼ PFA5 synthesized in *sc*-CO_2 and (B) the division example of PFA5. Curve a (experimental data) is deconvoluted into curves b (crystalline region at 2θ = 18.06°) and c (amorphous region at 2θ = 16.8°). The inset panel gives the fitted curves for PFA2 ∼ PFA5.

order whose polymer chains contain predominant successive TFE monomer units, and the other is in the much lower order where the molecular packing is interfered by perfluoropropyl side chains. That is why the more the PPVE content, the lower the second transition temperature is. It is also worth noting that the second lower transition peak becomes much broader with increased PPVE fraction, implying that the PPVE segments impact the crystallization of the copolymer main chains at various extents. The higher temperature transition peak becomes smaller with increased PPVE fraction, indicating that the block length of the TFE units gets shorter.

XRD measurements were also conducted for the copolymers, and the results are depicted in Figure 13. For PFA1 (0.4 mol % PPVE), a sharp peak at $2\theta = 18.06^\circ$ is observed. When more PPVE is incorporated, the peak becomes broader with depressed intensity, as can be seen from the XRD patterns for PFA2 $\sim$ PFA5 [Fig. 13(A)]. All the spectra exhibit a diffraction feature at $2\theta = 8$–22°. Similar to other TFE-based copolymers, such characteristic profile can be deconvoluted into two peaks at $2\theta = 18.06^\circ$ and 16.8°,[41,42] which are assignable to the crystalline and amorphous scatterings of the polymer chains. Figure 13(B) shows the division example of PFA-5; meanwhile, the fitted crystalline and amorphous peaks for PFA2 $\sim$ PFA5 are also shown in the inset panel. Clearly, the crystalline peak at $2\theta = 18.06^\circ$ becomes broader from PFA2 to PFA5, with gradually increased full width at half maximum (FWHM) from 1.017° to 1.355°, indicating the whole molecular arrangement of the crystalline chains getting less ordered with increasing PPVE content. It agrees well with the DSC result that the whole regularity of the highly regular and less ordered crystalline phases decreased with more PPVE fraction, as indicated by the increasingly lower and broader peak for the less order crystalline phase.

CONCLUSIONS

Copolymers of TFE and PPVE with perfluoroalkyl end groups were successfully synthesized by free radical polymerization using BPPP as an initiator in *sc*-CO_2. The reactivity ratios of TFE and PPVE in *sc*-CO_2 under different pressures were first reported. While r_{TFE} is about 8, r_{PPVE} is merely about 0.08, rendering TFE segments' predominant presence in the copolymer chains.

It is found that reaction pressure has a great impact on the monomer reactive ratios and copolymerization rates. Increasing the reaction pressure leads to the enhancement of the polarity for *sc*-CO_2, resulting in the increase of r_{TFE} and decrease of r_{PPVE}. Meanwhile, R_p increases with increasing the reaction pressure.

All polymers with varied compositions enjoy outstanding thermal stability. When the PPVE fraction in the copolymer is over 1 mol %, two transition peaks can be observed in the DSC thermogram, which are corresponding to the crystals with highly regular molecular arrangement or less-ordered chain packing which is disturbed by perfluoropropyl pendants. When more PPVE is incorporated, the whole regularity of the crystalline chains decreases, as indicated by the increasingly lower and broader peak of the less-ordered crystalline phase. Such conclusion is also confirmed by the XRD analysis.

We are grateful to Shandong Dongyue Polymer Materials Co. Ltd. for providing raw materials and sintered PTFE sample.

References

1. Chandy, T.; Das, G. S.; Wilson, R. F.; Rao, G. H. Biomaterials 2000, 21, 699.
2. Park, E.-S. J Appl Polym Sci 2008, 107, 372.
3. Carlson, D. P.; Schmiegel, W. Ullmann's Encyclopedia of Industrial Chemistry; John Wiley: New York, 1988.
4. Sperati, C. A. Handbook of Plastic Materials and Technology; John Wiley: New York, 1990.
5. Inoue, K.; Okada, F.; Ito, R.; Kato, S.; Sasaki, S.; Nakajima, S.; Uno, A.; Saijo, Y.; Sata, F.; Yoshimura, Y.; Kishi, R.; Nakazawa, H. Environ Health Perspect 2004, 112, 1204.
6. Bro, M. I.; Sperati, C. A.; J Polym Sci 1959, 38, 289.
7. Hintzer, K.; Lohr, G.; In Modern Fluoropolymer: High Performance Polymers for Diverse Applications; Scheirs, J., Ed.; John Wiley: New York, 1997; Chapter 11.
8. Du, L.; Kelly, J. Y.; Roberts, G. E.; DeSimone, J. M. J Supercrit Fluids 2009, 47, 447.
9. Toshiaki, M.; Yuri, T.; Yoshio, O. Macromolecules 2006, 39, 604.
10. Liu, T.; DeSimone, J. M.; Roberts, G. W. Polymer 2006, 47, 4276.
11. McHale, R.; Aldabbagh, F.; Zetterlund, P. B.; Okubo, M. Macromol Chem Phys 2007, 208, 1813.
12. Bramer, D. J.; Shiflett, M. B.; Yokozeki, A. S. U.S. Pat. 1993, 5,345,013.
13. Mccoy, M. Chem Eng New 1999, 77, 11.
14. Romack, T. J.; DeSimone, J. M. Macromolecules 1995, 28, 8429.
15. Romack, T. J.; DeSimone, J. M. U.S. Pat. 1997, 5,618,894.
16. Van Der Meer, R.; Aarts, M. W. A. M.; German, A. L. J Polym Sci Polym Chem Ed 1980, 18, 1347.
17. Lavrov, N. A. Russ J Appl Chem 2001, 74, 804.
18. Stassin, F.; Jérôme, R. Chem Commun 2003, 232.
19. Mori, T.; Tsuchiya, Y.; Okahata, Y. Macromolecules 2006, 39, 604.
20. Zhao, C. X.; Zhou, R. M.; Pan, H. Q.; Jin, X. S.; Qu, Y. L.; Wu, C. J.; Jiang, X. K. J Org Chem 1982, 47, 2009.
21. Wang, X.; Harris, H. R.; Bouldin, K.; Temkin, H.; Gangopadhyay, S.; Strathman, M. D.; West, M. J Appl Phys 2000, 87, 621.
22. Moynihan, R. E. J Am Chem Soc 1959, 81, 1045.
23. Lappan, U.; Geixler, U.; Scheler, U.; Lunkwitz, K. Radiat Phys Chem 2003, 67, 447.
24. Pianca, M.; Barchiesi, E.; Esposto, G.; Radice, S. J Fluorine Chem 1999, 95, 71.
25. Kushida, K.; Watanabe, A. Proton and fluorine nuclear magnetic resonance spectral data; 1988 ed. Varian Instruments Ltd. and Japan Halon Co., Tokyo 1988.

26. Dargaville, T. R.; George, G. A.; Hill, D. J. T.; Scheler, U.; Whittaker, A. K. Macromolecules 2002, 35, 5544.
27. Chen, Q.; Schmidt-Rohr, J. Macromolecules 2004, 37, 5995.
28. Lau, S. F.; Suzuki, H.; Wunderlich, B. J Polym Sci Polym Phys Ed 1984, 22, 379.
29. Bunyard, W. C.; Kadla, J. F.; DeSimone, J. M. J Am Chem Soc 2001, 123, 7199.
30. Ikeda, S.; Tabata, Y.; Suzuki, H.; Miyoshi, T.; Katsumura, Y. Radiat Phys Chem 2008, 77, 401.
31. Kelen, T.; Tüdös, F. J Macromol Sci Chem 1975, 9, 1.
32. Baradie, B.; Shoichet, M. S. Macromolecules 2002, 35, 3569.
33. Obriot, J.; Ge, J.; Bose, T. K.; St-Arnaud, J. M. Fluid Phase Equilib 1993, 86, 315.
34. Lebduška, J.; Šnupárek, J.; Kašpar, K.; Čermák, V. J Polym Sci Part A Polym Chem 1986, 24, 777.
35. Mayo, F. R.; Lewis, F. M. J Am Chem Soc 1944, 66, 1594.
36. Xu, A.; Zhao, J.; Yuan, W. Z.; Li, H.; Zhang, H.; Wang, L.; Zhang, Y. Macromol Chem Phys 2011, 212, doi: 10.1002/macp.201100126.
37. DeYoung, J. P.; Romack, T. J.; DeSimone, J. M. In Fluoropolymer: Synthesis; Hougham, G.; Cassidy, P. E.; Johns, K.; Davidson, T., Ed.; Kluwer Academic: New York, 2002; Vol. 1; Chapter 13.
38. Giaconia, A.; Scialdone, O.; Apostolo, M.; Filardo, G.; Galia, A. J Polym Sci Part A Polym Chem 2008, 46, 257.
39. Bunn, C. W.; Cobbold, A. J.; Palmer, R. P. J Polym Sci 1958, 28, 365.
40. Bunn, C. W.; Howells, E. R. Nature 1954, 174, 549.
41. Fujimura, M.; Hashimoto, T.; Kawai, H. Macromolecules 1981, 14, 1309.
42. Luan, Y.; Zhang, Y.; Zhang, H.; Li, L.; Li, H.; Liu, Y. J Appl Polym Sci 2008, 107, 396.